ACS OMEGA

http://pubs.acs.org/journal/acsodf

Article

# Novel Benzothiazole-Based Highly Selective Ratiometric Fluorescent Turn-On Sensors for $Zn^{2+}$ and Colorimetric Chemosensors for $Zn^{2+}$, $Cu^{2+}$, and $Ni^{2+}$ Ions

Chinna Ayya Swamy Pothulapadu,* Anjitha Jayaraj, Swathi N, Ragam N. Priyanka, and Gandhi Sivaraman

Cite This: *ACS Omega* 2021, 6, 24473−24483

Read Online

ACCESS | Metrics & More | Article Recommendations | Supporting Information

**ABSTRACT:** Metal ions play a very important role in environmental as well as biological fields. The detection of specific metal ions at a minute level caught much attention, and hence, several probes are available in the literature. Even though benzothiazole-based molecules have a special place in the medicinal field, only very few chemosensors are reported based on this moiety. The current work describes the design and synthesis of the benzothiazole-based chemosensor for a highly selective and sensitive detection of biologically important metal ions such as $Zn^{2+}$, $Cu^{2+}$, and $Ni^{2+}$. The sensing studies of **compound-1** showed a ratiometric as well as colorimetric response toward $Zn^{2+}$, $Cu^{2+}$, and $Ni^{2+}$ ions and color changes from colorless to yellow and is found to be insensitive toward various metal ions ($Cd^{2+}$, $Cr^{3+}$, $Mn^{2+}$, $Pb^{2+}$, $Ba^{2+}$, $Al^{3+}$, $Ca^{2+}$, $Fe^{2+}$, $Fe^{3+}$, $Mg^{2+}$, $K^{+}$, and $Na^{+}$). Further, **compound-1** exhibited ratiometric as well as *turn-on*-enhanced fluorescence response toward $Zn^{2+}$ ions and *turn off* response for $Cu^{2+}$ and $Ni^{2+}$ ions. The Job plots revealed that the binding stoichiometry of **compound-1** and metal ions is 2:1. The detection limits were found to be 0.25 ppm for $Zn^{2+}$, while it was 0.30 ppm and 0.34 ppm for $Ni^{2+}$ and $Cu^{2+}$, respectively. In addition, density functional theory results strongly support the colorimetric response of metals, and the reversibility studies suggested that **compound-1** can be used as a powerful chemosensor for the detection of $Zn^{2+}$, $Cu^{2+}$, and $Ni^{2+}$ ions. The bioimaging data illustrated that **compound-1** is a very effective ratiometric sensor for $Zn^{2+}$ ions in live cells.

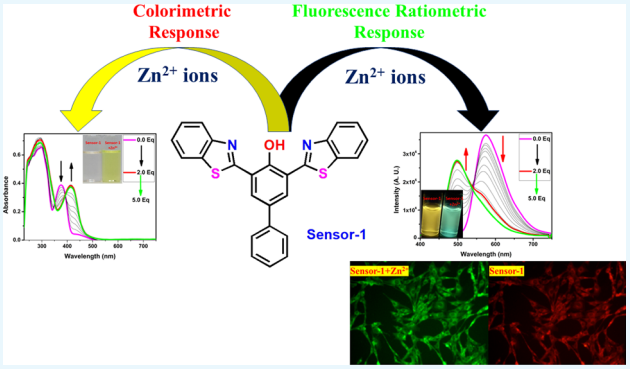


## INTRODUCTION

It is not surprising that in the advanced scientific era humans in an effort to ease their lives are unaware that their activities are harming nature and organisms. Importantly, the toxic metal ions, which harm the environment, have made us look back and think about the environmental concerns. Efforts are underway to find such toxic metal ions in the environment. Even though researchers have shown progress in this regard, more work is required to gain an upper hand in finding the toxic metal ions in the environment. The role of chemosensors in detecting the toxic metal ions in water bodies is outstanding.

Novel chemosensors continue to be an exciting area of the present research world. In the past, some traditional highly expensive instrumental methods such as atomic absorption spectroscopy,[1] inductively coupled plasma atomic emission,[2] anodic stripping voltammetry,[3a] potentiometry,[3b] spectrophotometry, and so on have been used for the detection of ions. Practically, these methods were considered to be unpropitious in terms of time consumption, need experts for the handling and cost.[4] Compared with the methods mentioned above, fluorescent chemosensors have drawn remarkable attention from the biological, chemical, and environmental research groups due to their ease of synthesis, high efficiency, selectivity, very fast response, low cost, as well as low detection limits toward metal ions particularly for transition-metal ions.[5] In addition to fluorescence enhancement or quenching, in some cases, the probe would also act as a colorimetric chemosensor for sensing the metal ions.[6] The colorimetric method of sensing is quick, equally selective and sensitive and associated with naked eye detection without the aid of any instrument. Colorimetric receptors have gained much attention, and researchers have focused on the synthesis of several artificial dyes for the selective recognition of specific metal ions.[6b,7] On the other hand, the development of highly sensitive ratiometric

Received: June 1, 2021
Published: September 15, 2021

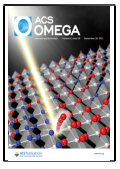

**Scheme 1. Synthetic Scheme for the Target Molecule**

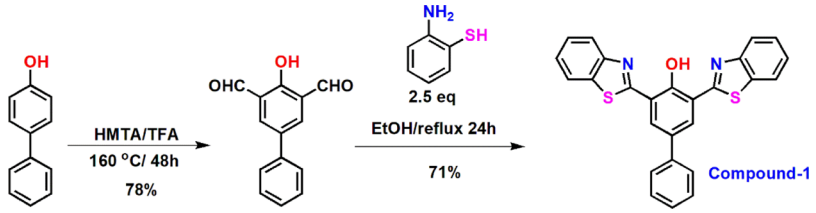


and "*turn-on*" fluorescent probes have superior significance due to their capability of detection of metal ions even in biological systems,[5b,6d,8] which was found to display different emission behavior upon metal binding. Due to the great impact on fluorescence *turn-on* receptors, lately, researchers have been devoted to the synthesis and structural modifications on BODIPY,[9] anthracene,[10] coumarin,[11] rhodamine,[12] and so on. However, several synthetic modifications on fluorescent dyes are found to have difficulties in purification and many of them lack the selectivity toward particular metal ions.

Zinc is the second most abundant metal in the human body and plays an important role in the biological reactions such as regulatory functions in enzyme catalysis, neurophysiology, gene expression, and DNA binding.[13] However, the imbalance of these metal ions can ultimately lead to neuron dysfunctions causing Alzheimer's, Parkinson's disease, amyotrophic lateral sclerosis, Creutzfeldt−Jakob disease, multisystem atrophy, diabetes, and prostate cancer.[14] Moreover, notably an excess of Zn leads to environmental pollution via the reduction of soil microbial activity causing phytotoxic effects.[15] Accordingly, due to the great relevance of Zn, it is very important to monitor its level in the biological system. Owing to the advantages and disadvantages of Zn, the design and synthesis of novel receptors which can detect and monitor its concentration have been a concern for chemists and are necessary. Moreover, recently, there have been several fluorescent receptors developed for the selective recognition of $Zn^{2+}$ ions such as chelating peptides, proteins, and macrocyclic compounds.[16]

Copper is the third most abundant transition-metal ion found in all body tissues after $Fe^{3+}$ and $Zn^{2+}$ owing to several essential biological processes. Moreover, copper is present in everything including soil, water, and air and is also an essential element for the all living beings such as human, animals, and plants.[17a] Several copper-containing pesticides and herbicides are extensively used for the treatment of plant diseases.[17b,c] Additionally, it plays an important role in the human body, for example, iron absorption, maintaining nerves, blood vessels, and active catalytical cofactor in several metalloenzymes, for instance, superoxide dismutase, tyrosinase, and cytochrome *c* oxidase.[18] However, the high amount of copper intake also becomes toxic to the body; destructive consequences causing irritation of the nose and throat, nausea, vomiting, and diarrhea. Further, a very high concentration of copper leads to the annihilation of organs in infants, whereas the deficiency of copper leads to abnormal growth of bones. The abnormal levels of copper lead to the disorder of the cellular homeostasis, which causes oxidative stress accompanied by several neurodegenerative syndromes, including Menkes, Wilson, familial amyotrophic lateral sclerosis, and Alzheimer's.[19]

Nickel is also an important trace element for a living system in respiration, biosynthesis, and metabolism.[20a] The deficiency of the nickel(II) ion leads to harmfulness to prokaryotic and eukaryotic organisms.[20] However, the accumulation of excessive nickel can cause lung cancer, asthma, sinus, pneumonitis, acute pneumonitis, syndromes of the central nervous system, and abnormal increment of blood cells.[21] In addition, $Ni^{2+}$ ions are also an environmental pollutant along with other heavy metal ions. Consequently, there is a very high demand for novel receptors of nickel in various chemical and biological samples.[22]

Even though numerous different types of chemosensors are available for the recognition of these biologically important metal ions ($Zn^{2+}$, $Cu^{2+}$, and $Ni^{2+}$), ratiometric, fluorescence *turn-on*, as well as colorimetric "naked eye" chemosensors have gained great attention due to their easy sample preparation, naked eye detection, effortlessness, high sensitivity, easy way of functioning, and usefulness of identifying metal ions in biological media via cellular imaging.[23] Additionally, the development of the single receptor, which could target multiple analytes, has been anomalously increasing in the past decade due to several advantages, such as potential cost and analytical time reduction. Recently, various research groups around the world focused on receptors which respond to multiple metal ions simultaneously, including $Cr^{3+}/Al^{3+}$,[24] $Cu^{2+}/Hg^{2+}$,[25] $Cu^{2+}/Zn^{2+}$,[26] $Zn^{2+}/Cd^{2+}$,[27] $Ag^{+}/Mn^{2+}$,[28] $Al^{3+}/Fe^{3+}$,[29] and $Cr^{3+}/Fe^{3+}$.[30]

In this context, we have proposed functionalized thiazole derivative compound **1** as a superior chemosensor for the recognition of $Zn^{2+}$, $Cu^{2+}$, and $Ni^{2+}$ with multiple binding sites such as N−O−N or S−O−S chelation. Heterocyclic compounds containing nitrogen and sulfur such as quinoline[31] and benzothiazole[32] correspondents were extensively studied in the field of the metal ion sensing chemistry as well as biological aspects. However, benzothiazole-based ratiometric and fluorescent *turn-on* chemosensors for $Zn^{2+}$ ions are scarce in the literature.[36] Herein, we have designed and synthesized biphenyl-based benzothiazole (**1**) via a condensation reaction between the 4-phenyl 2,6-diformylphenol and 2-aminobenzenethiol. The receptor was found to show a colorimetric response toward $Zn^{2+}$, $Cu^{2+}$, and $Ni^{2+}$ with a significant color change from colorless to yellow in DMSO/$CHCl_3$ (50:50, v/v) and no change upon the addition of other metal ions such as $Al^{3+}$, $Ca^{2+}$, $Cd^{2+}$, $Co^{2+}$, $Fe^{2+}$, $Fe^{3+}$, $Hg^{2+}$, $K^{+}$, $Mg^{2+}$, $Mn^{2+}$, $Na^{+}$, $Cd^{2+}$, and $Pb^{2+}$. Further, fluorescence titration of **1** was found to be ratiometric and fluorescence *turn-on* for $Zn^{2+}$, whereas *turn off* for $Cu^{2+}$ and $Ni^{2+}$. Moreover, the receptor showed the detection limit for $Zn^{2+}$ as low as 0.25 ppm and was very low as compared to $Ni^{2+}$ and $Cu^{2+}$ ions, which were 0.30 and 0.34 ppm, respectively.

## RESULTS AND DISCUSSION

The synthetic procedure for the new sensor is described as follows. First, 4-phenylphenol was treated with (hexamethylenetetramine) HMTA/(trifluoroacetic acid) TFA mixture and was refluxed for 48 h. The crude product was purified through


https://doi.org/10.1021/acsomega.1c02855
ACS Omega 2021, 6, 24473−24483

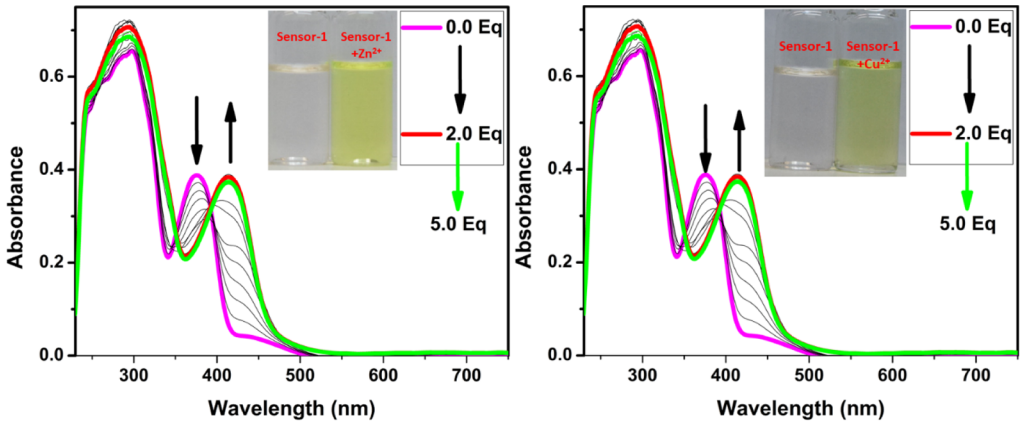


**Figure 1.** Change in absorption spectra of **compound-1** (1 $\mu$M) upon the addition of $Zn^{2+}$ (left) and $Cu^{2+}$ (right) in a 1:1 ratio of DMSO and $CHCl_3$ (inset photographs were taken in the presence of normal light).

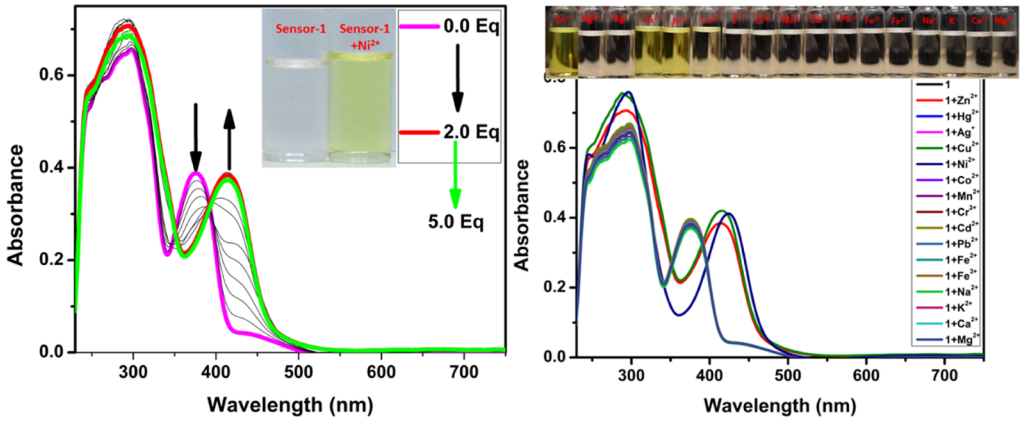


**Figure 2.** Change in absorption spectra of **compound-1** (1 $\mu$M) upon the addition of $Ni^{2+}$ (left) and different cations (right) in a 1:1 ratio of DMSO and $CHCl_3$ (inset photographs were taken in the presence of normal light).

column chromatography and the pure compound was obtained, 4-phenyl 2,6-diformylphenol as a yellow solid with 78% yield.[33] Further, the condensation reaction was carried out between 4-phenyl 2,6-diformylphenol and aminothiophenol in EtOH under reflux conditions for 24 h and a white compound was obtained as a target molecule with good yields, which was purified via column chromatography (Scheme 1).[32e] The target compound was structurally characterized by $^1H$, $^{13}C$ NMR, as well as high-resolution mass spectrometry (HRMS) (see in the Supporting Information).

After successfully obtaining the pure form of **compound-1**, we have evaluated the sensing ability toward diverse cations in a 1:1 ratio of DMSO and $CHCl_3$ solutions. The absorption spectrum of **compound-1** in DMSO displayed two strong bands around 300 and 370 nm, which can be attributed to $\pi-\pi^*$ and $n-\pi^*$ transitions, respectively. The metal ion sensing studies were carried out using UV−visible and fluorescence spectroscopic studies. 1 $\mu$M of **compound-1** was titrated with $Zn^{2+}$ ions and found that upon incremental addition, the absorption band at 370 nm was gradually decreased and simultaneously a new absorption band was generated at 440 nm. As a result, the color of the solution changed from colorless to dark yellow. Under similar conditions, $Ni^{2+}$ and $Cu^{2+}$ also showed similar changes in absorption bands, but a drastic change was seen in the case of $Ni^{2+}$ as compared with $Zn^{2+}$ and $Cu^{2+}$. Further, **compound-1** exhibited a ratiometric response toward $Ni^{2+}$, $Cu^{2+}$, and $Zn^{2+}$ (see the Supporting Information). The isosbestic point was found to be at 393 nm for $Zn^{2+}$, while for $Cu^{2+}$ and $Ni^{2+}$ were found to be at 392 and 405 nm, respectively, which clearly indicated the smooth molecular conversion of free ligand to metal complex. Therefore, the new bathochromic peaks can be accredited to the metal to ligand charge transfer, which is accountable for the naked eye detection of $Zn^{2+}$, $Cu^{2+}$, and $Ni^{2+}$ ions (Figures 1 and 2). Furthermore, we have checked the colorimetric response toward the other competitive metal ions such as $Cd^{2+}$, $Cr^{3+}$, $Mn^{2+}$, $Pb^{2+}$, $Ba^{2+}$, $Al^{3+}$, $Ca^{2+}$, $Fe^{2+}$, $Fe^{3+}$, $Mg^{2+}$, $K^+$, and $Na^+$, which caused no change or very slight change to the absorption spectra even in the presence of excess amounts of these metal ions.

The complete saturation of **compound-1** was obtained after the addition of 2.5 equiv of metal ions ($Ni^{2+}$, $Cu^{2+}$, and $Zn^{2+}$). Moreover, the binding stoichiometry of the receptor with metals ($Ni^{2+}$, $Cu^{2+}$, and $Zn^{2+}$) was determined using a Job's plot. This is an unceasing process as well as well known for the determination of the stoichiometric ratio of complexes. **Compound-1** displayed an absorption maximum around 440 nm upon the addition of metal ions, which was monitored for Job's plot to determine the ratios of compound-1 and metal ions. Various mole fractions of metal ions and **compound-1** were mixed in different proportions from 0.1, 0.2, 0.3, 0.4, 0.5, 0.6, 0.7, 0.8, and 0.9. The maximum absorbance for the complex was observed at 0.3 mole fraction corresponding to a 2:1 stoichiometry of the metal−**compound-1** complex


https://doi.org/10.1021/acsomega.1c02855
ACS Omega 2021, 6, 24473−24483

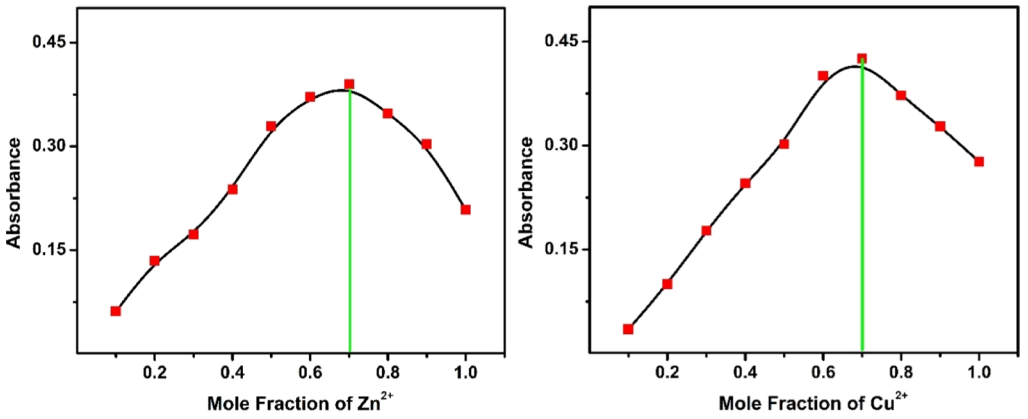


**Figure 3.** Job's plot according to the method of continuous variations, indicating the 1:2 stoichiometry for **compound-1** + $Zn^{2+}$ (left) and **compound-1** + $Cu^{2+}$ (right).

(Figures 3 and 4). Additionally, we have determined the association constants ($k_a$) of **compound-1** with $Zn^{2+}$, $Cu^{2+}$, and $Ni^{2+}$ ions which were found to be $4.9 \times 10^{11}$, $6.0 \times 10^{10}$, and $1.6 \times 10^{11} M^{-1}$, respectively. These results strongly suggested that the binding nature of $Zn^{2+}$ ions to the **compound-1** is much stronger as compared to $Cu^{2+}$ and $Ni^{2+}$ ions.

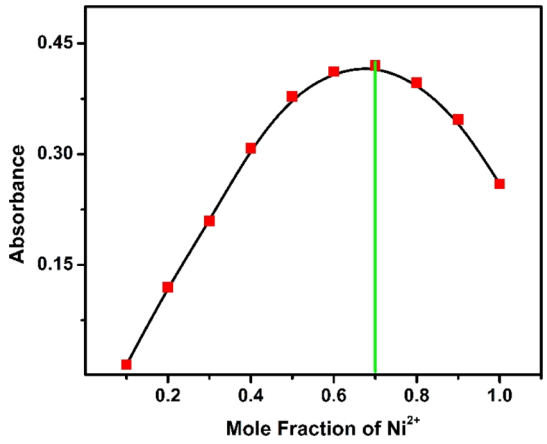


**Figure 4.** Job' plot according to the method of continuous variations, indicating the 1:2 stoichiometry for **compound-1** + $Ni^{2+}$ ions.

The fluorescence emission of **compound-1** exhibited a very bright yellow color (575 nm) with 0.55 quantum yields, upon excitation at 375 nm in a 1:1 ratio of DMSO and $CHCl_3$ solutions. To better understand the sensing ability of **compound-1**, we have carried out metal binding studies using fluorescence spectroscopy. During UV−visible titrations, we observed a color change in the solution as well as different fluorescence upon the addition of $Zn^{2+}$ ions. For better investigation, we have carried out the fluorescence titration of **compound-1** with the subsequent addition of $Zn^{2+}$ and found that the emission intensity at 575 nm was gradually decreased and consequently, a new emission band emerged at 520 nm. The ratiometric and fluorescence enhancement of **compound-1** witnessed the visual detection of $Zn^{2+}$ ions by the naked eye, when the samples were exposed to a UV lamp. The quantum yields of **compound-1** increased from 0.55 to 0.69 upon the binding of $Zn^{2+}$. Accordingly, **compound-1** could be utilized as an excellent *turn-on* fluorescence chemo receptor for $Zn^{2+}$ ions (Figure 5). On the other hand, the titration of $Cu^{2+}$ and $Ni^{2+}$ ions completely quenched the fluorescence intensity (Figures 5 and 6). The fluorescence quenching effect by $Cu^{2+}$ and $Ni^{2+}$ might be due to the presence of unpaired electrons and the energy-transfer process from the probe to the open shell d−orbitals of metal ions, which allows the non-radiation attenuation of the excited states to be more rapid and effective. The detection limit of **compound-1** toward $Zn^{2+}$, $Cu^{2+}$, and $Ni^{2+}$ was obtained using the calibration curve of emission versus composition, which is an important factor for a better

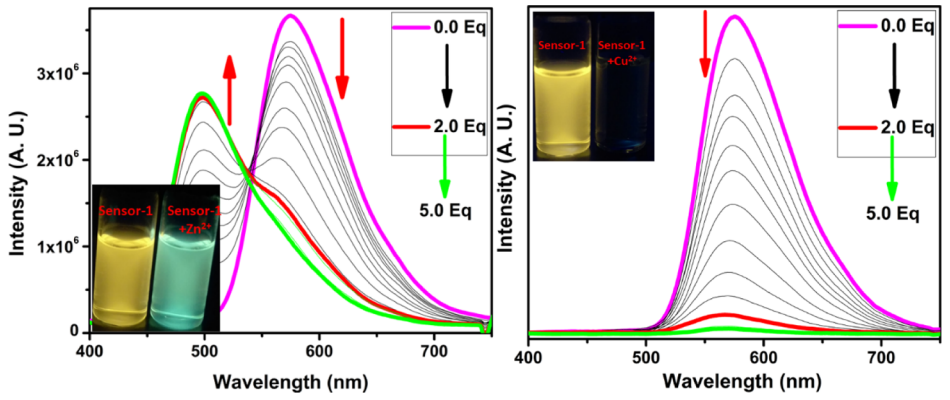


**Figure 5.** Change in emission spectra of **compound-1** (1 $\mu$M) upon the addition of $Zn^{2+}$ (left) and $Cu^{2+}$ (right) in a 1:1 ratio of DMSO and $CHCl_3$ (inset photographs were taken in the presence of UV light).



https://doi.org/10.1021/acsomega.1c02855
ACS Omega 2021, 6, 24473−24483

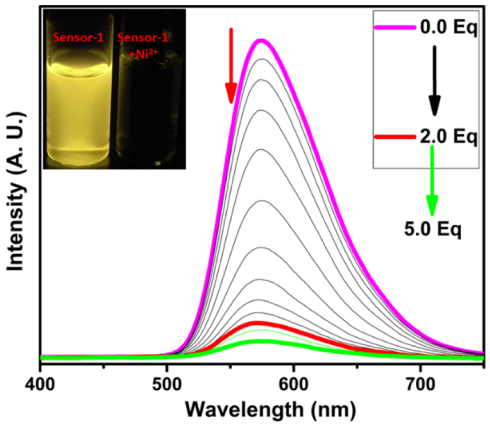


**Figure 6.** Change in emission spectra of **compound-1** (1 $\mu$M) upon the addition of $Ni^{2+}$ ions in a 1:1 ratio of DMSO and $CHCl_3$ (inset photographs were taken in the presence of UV light).

sensor and should be less than the limit set by the U.S. EPA (~20 $\mu$M or less) regulations.[34] The detection limits of **compound-1** toward metal ions, for example, $Zn^{2+}$, $Cu^{2+}$, and $Ni^{2+}$ were found to be as low as 0.25, 0.30, and 0.34 ppm, respectively. The quenching constant was calculated from the Stern−Volmer equation and found to be $2.0 \times 10^5$, $2.4 \times 10^5$, and $5.6 \times 10^5$ for $Zn^{2+}$, $Cu^{2+}$, and $Ni^{2+}$, respectively (Table S1). Further, the quenching efficiency of **compound-1** with $Zn^{2+}$, $Cu^{2+}$, and $Ni^{2+}$ was obtained to be 69, 96, and 98%, respectively, and further, the quantum yields of $Zn^{2+}$, $Cu^{2+}$, and $Ni^{2+}$ strongly supported the quenching efficiency (see the Supporting Information). From these results, one can conclude that the quenching efficiency and quenching constant for $Ni^{2+}$ is high as compared with that of $Zn^{2+}$ and $Cu^{2+}$ ions.

Furthermore, we explored the sensitivity and selectivity of **compound-1** toward several metal ions and was compared with $Zn^{2+}$. A 1 $\mu$M stock solution of **compound-1** in a 1:1 ratio of DMSO and $CHCl_3$ solutions was treated with excess amounts of diverse metal ions such as $Cd^{2+}$, $Cr^{3+}$, $Mn^{2+}$, $Pb^{2+}$, $Ba^{2+}$, $Al^{3+}$, $Ca^{2+}$, $Fe^{2+}$, $Fe^{3+}$, $Mg^{2+}$, $K^+$, and $Na^+$ for the investigation of selectivity. **Compound-1** exhibited high selectivity and ratiometric as well as fluorescence *turn-on* response toward $Zn^{2+}$, while $Cu^{2+}$ and $Ni^{2+}$ metal ions displayed fluorescence *turn-off*, other metal ions do not influence the emission spectra (Figure 7).

In addition, competitive selectivity of **compound-1** with respect to $Zn^{2+}$ in the presence of other interfering candidates such as $Cu^{2+}$, $Ni^{2+}$, $Cd^{2+}$, $Cr^{3+}$, $Mn^{2+}$, $Pb^{2+}$, $Ba^{2+}$, $Al^{3+}$, $Ca^{2+}$, $Fe^{2+}$, $Fe^{3+}$, $Mg^{2+}$, $K^+$, and $Na^+$ was studied. The initial emission band of **compound-1** with excess amounts of various other metal ions exhibited very low and constant intensity which upon the addition of 5 equiv of $Zn^{2+}$ led to efficient enhancement of green emission with good quantum yields (Figure 7). These results strongly suggest the excellent selectivity of **compound-1** for $Zn^{2+}$ ions in the presence of other mentioned interfering metal ions.

To get an insight into the photophysical responses of the **compound-1** with metal ions, we carried out the quantum mechanical calculations of the free probe and its metal coordinated complexes with the help of density functional theory (DFT) method using a Gaussian 09 program[35] at the level of B3LYP/631G/LANL2DZ (d,p) for C, H, N, S, O, and metal ions ($Zn^{2+}$, $Cu^{2+}$, and $Ni^{2+}$). The energy minimized structure of **compound-1** and **compound-1**−$Zn^{2+}$ complexes is shown in Figure 8, whereas for complexes of $Cu^{2+}$ and $Ni^{2+}$ are given in the Supporting Information.

In addition, the frontier molecular orbitals reveal that **compound-1** as well as metal complexes of $Zn^{2+}$, $Cu^{2+}$, and $Ni^{2+}$ will provide the valuable information about electronic transitions. Using the optimized structures, time-dependent DFT (TDDFT) calculations were carried out and created a checkpoint file which was used to generate frontier molecular orbital cubes. The highest occupied molecular orbital (HOMO) and lowest unoccupied molecular orbital (LUMO) of **compound-1** were mostly concentrated on the whole $\pi$-moiety of benzothiazole as well as biphenyl units with

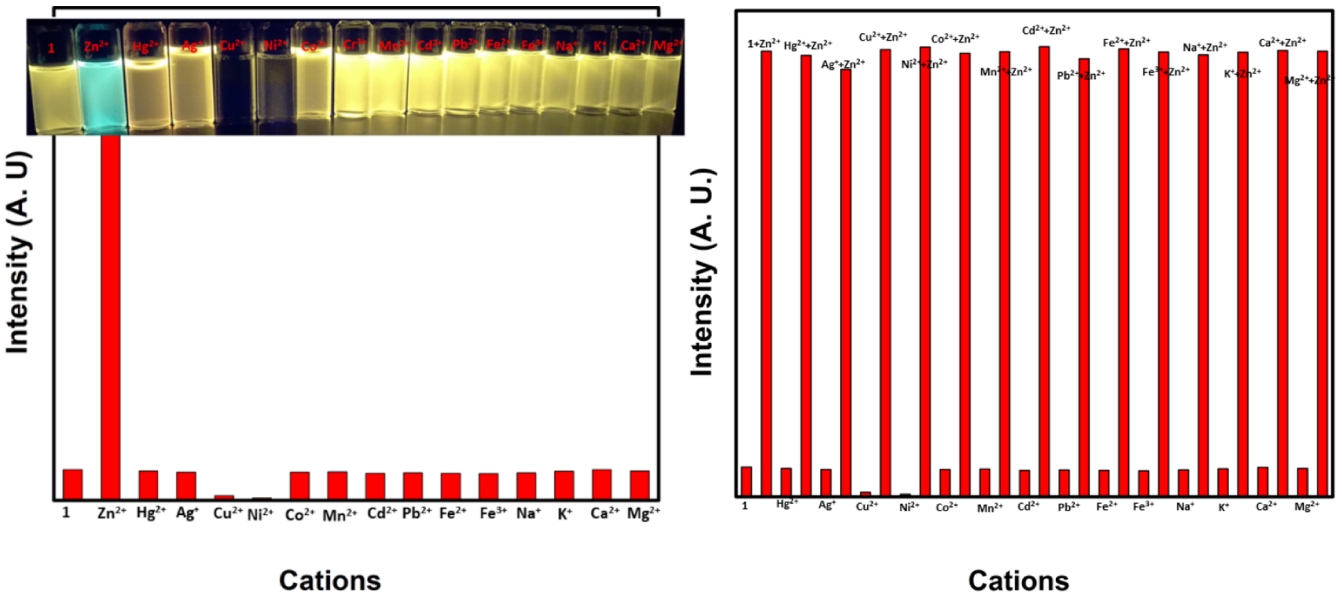


**Figure 7.** Examination of selectivity (left) and competitive (right) studies of **compound-1** (1 $\mu$M) toward various metal ions. The competitive binding ability of **compound-1** (1 $\mu$M) were observed toward $Zn^{2+}$ in the presence of other interfering metal ions and the emission band was monitored at 520 nm. Inset photographs were taken in UV light.



https://doi.org/10.1021/acsomega.1c02855
ACS Omega 2021, 6, 24473−24483

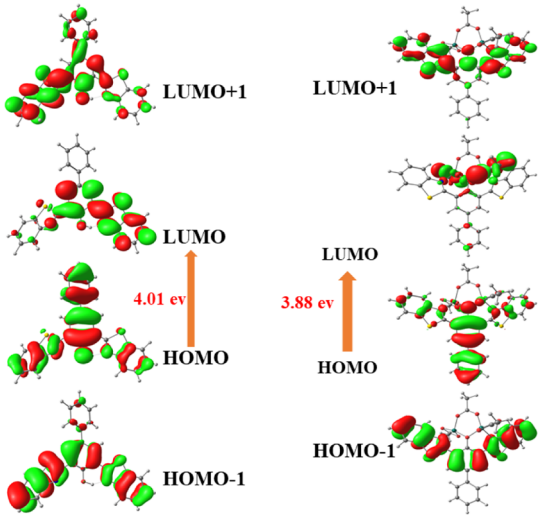


**Figure 8.** Selected MOs of **compound-1** and **compound-1** + $Zn^{2+}$ (not to scale; isovalue = 0.02).

a HOMO−LUMO gap of 4.02 eV, which indicated the transition of $\pi$ to $\pi^*$ of the benzothiazole unit. As evident from UV−visible and fluorescence titration spectra, the stoichiometry of **compound-1** and $Zn^{2+}$, $Cu^{2+}$, and $Ni^{2+}$ was confirmed strongly as 1:2 and hence, the optimization of the metal complex was carried out with 1:2 coordinated complexes taking acetate as an auxiliary ligand and optimized using LAN2DZ basis sets. In the **compound-1−$Zn^{2+}$** complex, the HOMO is situated completely on the whole biphenyl−benzothiazole moiety, whereas LUMO is spread over $Zn^{2+}$ ions with a band gap of 3.88 eV (Figure 6). These results clearly revealed the interruption of internal charge transfer after the appendage of $Zn^{2+}$ ions to **compound-1**. Similarly, the calculated HOMO−LUMO gap of other metal complexes ($Cu^{2+}$ and $Ni^{2+}$) were small compared to that of **compound-1**. These findings intensely supported the reason for the colorimetric response upon the addition of metal ions ($Zn^{2+}$, $Cu^{2+}$, and $Ni^{2+}$) to **compound-1**.

Furthermore, the TDDFT of **compound-1** and metal complexes ($Zn^{2+}$, $Cu^{2+}$, and $Ni^{2+}$) were carried out in the LAN2DZ basis set to investigate the electronic transition in absorption spectra in vacuum. Further, the compared oscillator strength of **compound-1** and its metal complexes provided the valuable evidence for the colorimetric response. It was noticed that the absorption spectrum of **compound-1** consists of two major peaks at 295 and 375 nm with energies 3.8894904 and 4.480113 eV for the key electron transitions, respectively. However, TDDFT data showed two major strong bands at 389.37 and 279.24 nm with energies of 3.1842 and 4.4401 eV correspondingly. As evident from TDDFT data, the absorption bands of the $Zn^{2+}$ complex displayed at 411.32 and 309.69 nm and the strong absorption band in the visible region are attributed to intraligand charge-transfer bands, which also matched with the experimental data. These outcomes are strongly supported by the oscillator strength of **compound-1** before and after metal complexes with a change from 0.2110 to 1.8996. The formation of the metal ion complex with **compound-1** had gradually enhanced the absorption band in the visible region, which might be due to the change in electronic transition and marginal sensitivity of the metal ions. For example, **compound-1** and its complexation with $Zn^{2+}$ was found to give a bathochromic shift with 40 nm as noted in UV−visible spectra. On the other hand, the resultant $Ni^{2+}$ complex led to a huge bathochromic shift in the absorption of ($\Delta\lambda$) 52 nm and $Cu^{2+}$ prompts instead similar red shifts ($\Delta\lambda \approx$ 42 nm) as compared with $Zn^{2+}$. Further, these arguments are completely supported by the change in energy gap values, which are observed from DFT studies. In addition, we carried out DFT/TDDFT calculations of **compound-1−$Cu^{2+}$** and **compound-1−$Ni^{2+}$** complexes under similar conditions and found that the oscillator strength values were relatively unchanged compared with **compound-1−$Zn^{2+}$**. Also, these data provided further evidence for the observed selectivity of the **compound-1** with **$Zn^{2+}$**.

The strong affinity of **compound-1** toward $Zn^{2+}$ and the ratiometric response of **compound-1** encouraged us to explore the applicability of **compound-1** for the ratiometric fluorescence imaging of $Zn^{2+}$ ions in live cells. Initially, the cytotoxicity of **compound-1** toward HeLa cells was studied by the standard MTT assay, explaining the least cytotoxic nature to the cells. Further, HeLa cells were cultured in Dulbecco's modified Eagle medium (DMEM) and the cells were incubated with **compound-1** for 30 min at 25 °C. Later, the cells were imaged through a fluorescence microscope, a high red fluorescence was observed only inside the cellular regions and was clearly supported by the ICT mechanism in biological samples also. Furthermore, 10 $\mu$M of $Zn^{2+}$ solution (DMEM) was added prior to the incubation and was kept for 10 min. Later, the cells were washed with PBS buffer solutions to remove an excess amount of $Zn^{2+}$ ions and were subjected to fluorescence microscopy imaging and the bright green emission was observed inside the cells (Figure 9). From these results, one can conclude that **compound-1** could be a promising candidate for the practical protocol in ratiometric imaging of living cells in biology.

A good sensor should exhibit better selectivity as well as reversibility nature; thus, we have examined the reversibility of **compound-1** with $Zn^{2+}$ in a 1:1 ratio of DMSO and $CHCl_3$ solutions. Upon the addition of 5 equiv of the EDTA solution to the $Zn^{2+}$ + **compound-1** solution; the original emission of

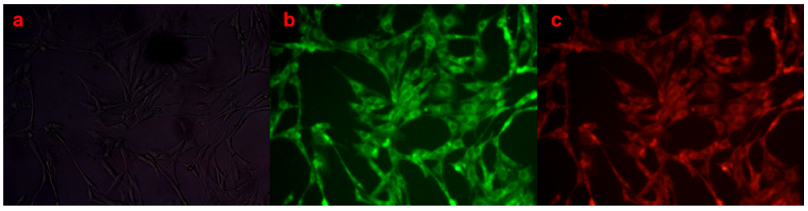


**Figure 9.** Cellular images of $Zn^{2+}$ ions in HeLa cell lines at 37 °C (a) bright field image of **compound-1** + $Zn^{2+}$ ion-treated HeLa cells; (b) fluorescence imaging of HeLa cells with **compound-1** after 10 min of treatment of 10 $\mu$M $Zn^{2+}$ ions; and (c) HeLa cells incubated with **compound-1** for 30 min.



https://doi.org/10.1021/acsomega.1c02855
ACS Omega 2021, 6, 24473−24483

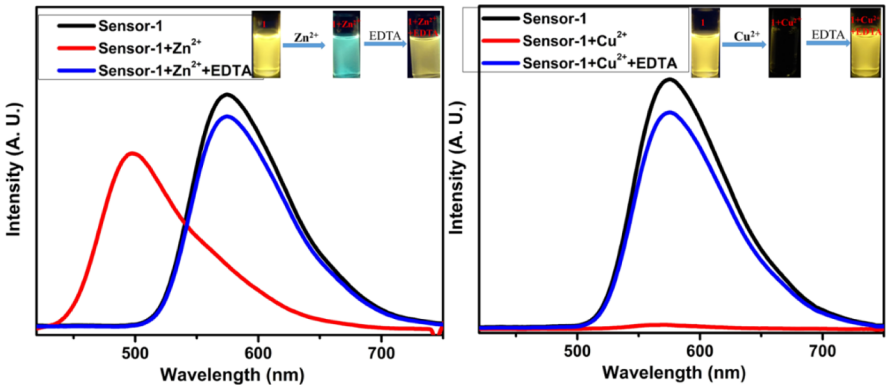


**Figure 10.** Reversibility studies of **compound-1** upon the addition of EDTA to **compound-1** + $Zn^{2+}$ (left) and **compound-1** + $Cu^{2+}$ (right).

**compound-1** was regenerated (Figure 10), which indicated that the EDTA was involved in captivating the $Zn^{2+}$ ion. $Cu^{2+}$ and $Ni^{2+}$ complexes with **compound-1** also furnished the same results (Figures 10 and 11). These experiments strongly confirm that **compound-1** has very good reversibility and thus, it can be employed as a useful and better chemosensor probe selectively for $Zn^{2+}$ ions.

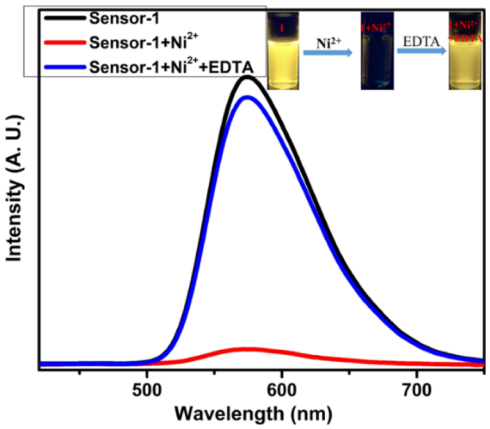


**Figure 11.** Reversibility studies of **compound-1** upon the addition of EDTA to **compound-1** + $Ni^{2+}$.

## CONCLUSIONS

In summary, we have designed and synthesized a biphenyl−benzothiazole-based chemosensor and was characterized by $^{1}H$, $^{13}C$ NMR, as well as HRMS. The novel sensor exhibited ratiometric and colorimetric responses toward biologically important metal ions such as $Zn^{2+}$, $Cu^{2+}$, and $Ni^{2+}$ with significant color changes from colorless to yellow in DMSO/$CHCl_3$ (50:50, v/v) over other metal cations ($Cd^{2+}$, $Cr^{3+}$, $Mn^{2+}$, $Pb^{2+}$, $Ba^{2+}$, $Al^{3+}$, $Ca^{2+}$, $Fe^{2+}$, $Fe^{3+}$, $Mg^{2+}$, $K^{+}$, and $Na^{+}$). Further, fluorescence studies revealed that there was an enhanced fluorescence in the emission spectra, upon the addition of $Zn^{2+}$ ions and that make **compound-1** as a potential ratiometric as well as fluorescence *turn-on* chemosensor, which was strongly supported by the elevating quantum yields, whereas a *turn-off* chemosensor for $Cu^{2+}$ and $Ni^{2+}$ ions. The selectivity and competitive studies also strongly suggested that **compound-1** was excellent for $Zn^{2+}$ ions in the presence of other mentioned interfering metal ions. Moreover, **compound-1** showed the detection limit for $Zn^{2+}$ ions as 0.25 ppm which was lower compared to that of $Ni^{2+}$ and $Cu^{2+}$ ions which were 0.30 and 0.34 ppm, respectively. The binding stoichiometry of the metal complex was determined using a Job's plot and was found to be 1:2 for **compound-1** with all the three metal ions. The reversibility of **compound-1** was studied upon the addition of EDTA and found that the green color emission of **compound-1** was changed to yellow, restoring the emission of **compound-1**, proving the reversibility of the chemosensor. Similarly, metal complexes of **compound-1** with $Ni^{2+}$ and $Cu^{2+}$ ions follow similar trends of $Zn^{2+}$ ions. The ratiometric response of **compound-1** toward $Zn^{2+}$ ions extend its applicability in the fluorescence cellular imaging of $Zn^{2+}$ ions in live cells and found a color change from red to green fluorescence in cells. Due to the presence of these novel properties, **compound-1** can act as an excellent chemosensor for the detection of biologically important metal ions such as $Zn^{2+}$, $Cu^{2+}$, and $Ni^{2+}$ in the environment as well as bioimaging ($Zn^{2+}$ ions) of live cells.

## EXPERIMENTAL SECTION

All reagents were of analytical grade and used without further purification, otherwise noted the purification process. Glassware was oven dried at 140 °C for at least 2 h prior to use and allowed to cool under vacuum. 4-Phenylphenol, aminothiophenol, (Alfa Aesar), TFA, EtOH, MeOH, diethylether, and DMSO (Spectrochem). HMTA and all the metal salts were used as such without purification (Merck India). Flash chromatography was carried out on Merck Kieselgel 60 (230−400 mesh) as the stationary phase under a positive pressure using AR grade solvents; the procedure includes the removal of solvents under reduced pressure. Thin-layer chromatography was performed on precoated Merck Kieselgel silica gel plates (60 F254, Merck, Germany) monitored by UV light and iodine. Electrospray ionization time-of-flight mass spectrometry (TOF MS ES+) and HRMS were recorded on a Waters QTOFMS Xevo G2 spectrometer in the positive ion mode. The $^{1}H$, $^{13}C\{^{1}H\}$ NMR were recorded on a Bruker AVANCE III 400 MHz NMR spectrometer. All solution $^{1}H$ and $^{13}C$ spectra were referenced internally to the solvent signal (TMS). In rare instances where other NMR solvents have been used, an appropriate mention has been made in the text. Chemical shifts are expressed in parts per million (ppm) and coupling constants ($J$) are in Hz. The $^{1}H$ and $^{13}C\{^{1}H\}$ NMR spectra were referenced using residual H impurities in the deuterated solvents. Deuterated solvents ($CDCl_3$) were purchased from Cambridge Isotope Laboratories, dried over calcium hydride, degassed by three freeze−pump−thaw cycles, and vacuum-transferred prior to use. Electronic absorption spectra were


https://doi.org/10.1021/acsomega.1c02855
ACS Omega 2021, 6, 24473−24483

recorded on a PerkinElmer LAMBDA 750 UV/visible spectrophotometer. The solutions were prepared using a microbalance (±0.1 mg) and volumetric glassware and then charged in quartz cuvettes with sealing screw caps. Fluorescence emission studies were carried out on a Horiba JOBIN YVON Fluoromax-4 spectrometer. All aqueous solutions were prepared with double distilled deionized water. The standard stock solution of $Ag^{+}$, $Co^{2+}$, $Pb^{2+}$, $Zn^{2+}$, $Cd^{2+}$, $Cr^{3+}$, $Mn^{2+}$, $Pb^{2+}$, $Ba^{2+}$, $Al^{3+}$, $Ca^{2+}$, $Fe^{2+}$, $Fe^{3+}$, $Mg^{2+}$, $K^{+}$, $Cu^{2+}$, $Na^{+}$, $Cd^{2+}$, and $Hg^{2+}$ was prepared by dissolving their nitrate salts.

**Synthesis of 4-Phenyl 2,6-Diformylphenol (A).**

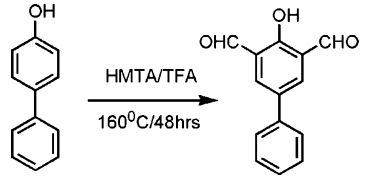


4-Phenylphenol (5 g, 29 mmol) was dissolved in TFA (100 mL). Hexamethylene tetramine (32 g, 232 mmol) was added to the solution and refluxed at 160 °C for 48 h (Scheme 1). The reaction mixture was stirred in 6 N HCl (100 mL) for 30 min. The crude reaction mixture was extraction with DCM and purified through silica gel column chromatography (2:8 ratios of ethyl acetate and hexanes). A yellow colored powder was obtained with yield 78%. $^1$H NMR (400 MHz, $CDCl_3$) $\delta$ 11.63 (s, 1H), 10.32 (s, 2H), 8.19 (s, 2H), 7.59 (d, $J$ = 7.3 Hz, 2H), 7.48 (t, $J$ = 7.5 Hz, 2H), 7.41 (d, $J$ = 7.3 Hz, 1H) (the $^1$H NMR data was matching with literature reports). HRMS (EI): calcd for $C_{14}H_{10}NaO_3$ $[M + Na]^+$ $m/z$, 249.0528; found $m/z$, 249.0532.

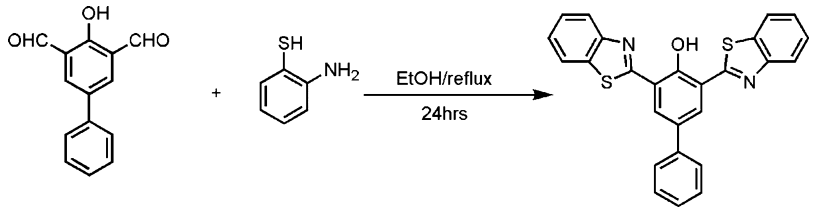


**Synthesis of Compound-1.** A stirred mixture of 4-phenyl 2,6-diformylphenol (0.5 g, 2.2 mmol) and aminothiophenol (0.7 g, 5.5 mmol) in 60 mL of EtOH was refluxed for 24 h. The crude product was purified by column chromatography using silica gel and solvent was dried under vacuum. A dirty white product was obtained with 71% yield. $^1$H NMR (400 MHz, $CDCl_3$): $\delta$ 14.24 (s, 1H), 8.48 (s, 2H), 8.10 (d, $J$ = 8.0 Hz, 2H), 7.98 (d, $J$ = 7.5 Hz, 2H), 7.80−7.71 (m, 2H), 7.61−7.48 (m, 4H), 7.49−7.39 (m, 3H). $^{13}$C NMR (101 MHz, $CDCl_3$): $\delta$ 155.6, 151.8, 139.6, 133.2, 128.9, 127.5, 127.1, 126.6, 125.5, 122.6, 121.6, 116.7. HRMS (EI): calcd for $C_{26}H_{17}N_2OS_2$ $[M + H]^+$ $m/z$, 437.0782; found $m/z$, 437.0780.

## ■ ASSOCIATED CONTENT

### Supporting Information

The Supporting Information is available free of charge at https://pubs.acs.org/doi/10.1021/acsomega.1c02855.

$^1$H NMR, $^{13}$C NMR, HRMS, and characterization data for all the compounds, photophysical data, association constants, detection limits, and DFT results (PDF)

## ■ AUTHOR INFORMATION


### Corresponding Author

**Chinna Ayya Swamy Pothulapadu** − *Main Group Organometallics Materials, Supramolecular Chemistry and Catalysis Lab, Department of Chemistry, National Institute of Technology, Calicut 673601, India;* orcid.org/0000-0001-7875-9517; Email: swamy@nitc.ac.in

### Authors

**Anjitha Jayaraj** − *Main Group Organometallics Materials, Supramolecular Chemistry and Catalysis Lab, Department of Chemistry, National Institute of Technology, Calicut 673601, India*

**Swathi N** − *Maharani Lakshmi Ammanni College for Women (Autonomous), Bangalore 560012, India*

**Ragam N. Priyanka** − *School of Chemical Sciences, Mahatma Gandhi University, Kottayam 686560, India*

**Gandhi Sivaraman** − *Department of Chemistry, Gandhigram Rural Institute (Deemed to be University), Gandhigram 624302, India;* orcid.org/0000-0002-6919-9658

Complete contact information is available at: https://pubs.acs.org/10.1021/acsomega.1c02855


### Notes

The authors declare no competing financial interest.

## ■ ACKNOWLEDGMENTS

C.A.S.P thanks the Department of Chemistry at National Institute of Technology, Calicut, for the financial support. A.J. thanks National Institute of Technology, Calicut, for Institute-JRF fellowship. C.A.S.P thanks to Dr. Parameswaran P. for the use of his computational work station.

## ■ REFERENCES

(1) Mirzaei, M.; Behzadi, M.; Abadi, N. M.; Beizaei, A. Simultaneous separation/preconcentration of ultra-trace heavy metals in industrial wastewaters by dispersive liquid−liquid microextraction based on solidification of floating organic drop prior to determination by graphite furnace atomic absorption spectrometry. *J. Hazard. Mater.* **2011**, *186*, 1739−1743.

(2) Sitko, R.; Janik, P.; Zawisza, B.; Talik, E.; Margui, E.; Queralt, I. Green Approach for Ultratrace Determination of Divalent Metal Ions and Arsenic Species Using Total-Reflection X-ray Fluorescence Spectrometry and Mercapto-Modified Graphene Oxide Nanosheets as a Novel Adsorbent. *Anal. Chem.* **2015**, *87*, 3535−3542.

(3) (a) Curdová, E.; Vavrusková, L.; Suchánek, M.; Baldrian, P.; Gabriel, J. ICP-MS determination of heavy metals in submerged cultures of wood-rotting fungi. *Talanta* **2004**, *62*, 483−487. (b) Petrović, S.; Guzsvany, V.; Ranković, N.; Beljin, J.; Rončević, S.; Dalmacija, B.; Ashrafi, A. M.; Konya, Z.; Švancara, I.; Vytřas, K. Trace level voltammetric determination of Zn(II) in selected nutrition

related samples by bismuth-oxychloride-multiwalled carbon nanotube composite based electrode. *Microchem. J.* **2018**, *146*, 178−186.
(4) (a) Li, S.; Zhang, C.; Wang, S.; Liu, Q.; Feng, H.; Ma, X.; Guo, J. Electrochemical microfluidics techniques for heavy metal ion detection. *Analyst* **2018**, *143*, 4230−4246. (b) Li, Y.; Chen, Y.; Yu, H.; Tian, L.; Wang, Z. Portable and smart devices for monitoring heavy metal ions integrated with nanomaterials. *TrAC, Trends Anal. Chem.* **2018**, *98*, 190−200.
(5) (a) Sahoo, S. K.; Sharma, D.; Bera, R. K.; Crisponi, G.; Callan, J. F. Iron(iii) selective molecular and supramolecular fluorescent probes. *Chem. Soc. Rev.* **2012**, *41*, 7195−7227. (b) Carter, K. P.; Young, A. M.; Palmer, A. E. Fluorescent sensors for measuring metal ions in living systems. *Chem. Rev.* **2014**, *114*, 4564−4601. (c) Jiang, P.; Guo, Z. Fluorescent detection of zinc in biological systems: recent development on the design of chemosensors and biosensors. *Coord. Chem. Rev.* **2004**, *248*, 205−229.
(6) (a) Baljeet, K.; Navneet, K.; Subodh, K. Colorimetric metal ion sensors − A comprehensive review of the years 2011−2016. *Coord. Chem. Rev.* **2018**, *358*, 13−69. (b) Ali, Q. A.; Mohamed, A.; Sami, A. Z. Colorimetric Detection of Multiple Metal Ions Using Schiff Base 1-(2-Thiophenylimino)-4-(N-dimethyl)benzene. *Chemosensors* **2020**, *8*, 1−10. (c) Hao, Z.; Jiangli, F.; Benhua, W.; Xiaojun, P. Fluorescent, MRI, and colorimetric chemical sensors for the first-row d-block metal ions. *Chem. Soc. Rev.* **2015**, *44*, 4337−4366. (d) Sanchari, P.; Nabanita, C.; Parimal, K. B. Selectively sensing first-row transition metal ions through fluorescence enhancement. *RSC Adv.* **2014**, *4*, 26585−26620. (e) Erdemir, S.; Malkondu, S. Calix[4]arene based a NIR-fluorescent sensor with an enhanced stokes shift for the real-time visualization of Zn(II) in living cells. *Sens. Actuators, B* **2020**, *306*, 127574.
(7) Shalini, U.; Ajay, S.; Riya, S.; Shivangi, O.; Kiran, N. Colorimetric chemosensors for d-metal ions: A review in the past, present and future prospect. *J. Mol. Struct.* **2019**, *1193*, 89−102. (b) Jung, J. M.; Lee, S. Y.; Kim, C. A novel colorimetric chemosensor for multiple target metal ions $Fe^{2+}$, $Co^{2+}$, and $Cu^{2+}$ in a near-perfect aqueous solution: experimental and theoretical studies. *Sens. Actuators, B* **2017**, *251*, 291−301.
(8) (a) Luo, A.; Wang, H.; Wang, Y.; Huang, Q.; Zhang, Q. A novel colorimetric and turnon fluorescent chemosensor for iron(III) ion detection and its application to cellular imaging. *Spectrochim. Acta, Part A* **2016**, *168*, 37−44. (b) Yuan, L.; Lin, W.; Zheng, K.; Zhu, S. FRET-based small-molecule fluorescent probes: rational design and bioimaging applications. *Acc. Chem. Res.* **2013**, *46*, 1462−1473. (c) Guo, Z.; Hu, T.; Sun, T.; Li, T.; Chi, H.; Niu, Q. A colorimetric and fluorimetric oligothiophene-indenedione-based sensor for rapid and highly sensitive detection of cyanide in real samples and bioimaging in living cells. *Dyes Pigm.* **2019**, *163*, 667−674.
(9) (a) Ahmed, N. K.; Elif, B.; Ersin, G. Importance of BODIPY-based Chemosensors for Cations and Anions in Bio-imaging Applications, *Curr. Anal. Chem.* **2020**, *17*, DOI: 10.2174/1573411017666201215105055; (b) Apurba, M.; Utsav, G.; Dipanjan, G.; Devdeep, M.; Tapas, K. M.; Sanjib, K. P. A water-soluble BODIPY based 'OFF/ON' fluorescent probe for the detection of $Cd^{2+}$ ions with high selectivity and sensitivity. *Dalton Trans.* **2019**, *48*, 2108−2117.
(10) (a) Chinna Ayya Swamy, P.; Jeyabalan, S.; Subramanian, S.; Sivaraman, G.; Duraisamy, C. Anthracene-Based Highly Selective and Sensitive Fluorescent "Turn-on" Chemodosimeter for $Hg^{2+}$. *ACS Omega* **2018**, *3*, 12341−12348. (b) Kaur, N.; Kaur, B. Recent development in anthracene possessing chemosensors for cations and anions. *Microchemical Journal* **2020**, *158*, 105131.
(11) Duxia, C.; Zhiqiang, L.; Peter, V.; Seyoung, K.; Paramesh, J.; Jong, S. K.; Weiying, L. Coumarin-Based Small-Molecule Fluorescent Chemosensors. *Chem. Rev.* **2019**, *119*, 10403−10519.
(12) (a) Ha, N. K.; Min, H. L.; Hyun, J. K.; Jong, S. K.; Juyoung, Y. A new trend in rhodamine-based chemosensors: application of spirolactam ring-opening to sensing ions. *Chem. Soc. Rev.* **2008**, *37*, 1465−1472. (b) Ruiqi, Z.; Fanyong, Y.; Yicun, H.; Depeng, K.; Qianghua, Y.; Jinxia, X.; Li, C. Rhodamine-based ratiometric fluorescent probes based on excitation energy transfer mechanisms: construction and applications in ratiometric sensing. *RSC Adv.* **2016**, *6*, 50732−50760.
(13) (a) Berg, J. M.; Shi, Y. The galvanization of biology: a growing appreciation for the roles of zinc. *Science* **1996**, *271*, 1081−1085. (d) Frederickson, C. J.; Koh, J.-Y.; Bush, A. I. The neurobiology of zinc in health and disease. *Nat. Rev. Neurosci.* **2005**, *6*, 449−462. (e) Fraker, P. J.; King, L. E. Reprogramming of the immune system during zinc deficiency. *Annu. Rev. Nutr.* **2004**, *24*, 277−298. (f) Que, E. L.; Domaille, D. W.; Chang, C. J. Metals in neurobiology: probing their chemistry and biology with molecular imaging. *Chem. Rev.* **2008**, *108*, 1517. (g) Suhy, D. A.; Simon, K. D.; Linzer, D. I. H.; O'Halloran, T. V. Metallothionein is part of a zincscavenging mechanism for cell survival under conditions of extreme zinc deprivation. *J. Biol. Chem.* **1999**, *274*, 9183−9192.
(14) (a) Bush, A. I. The metallobiology of Alzheimer's disease. *Trends Neurosci.* **2003**, *26*, 207−214. (b) Strausak, D.; Mercer, J. F. B.; Dieter, H. H.; Stremmel, W.; Multhaup, G. Copper in disorders with neurological symptoms: Alzheimer's, Menkes, and Wilson diseases. *Brain Res. Bull.* **2001**, *55*, 175−185. (c) Rolfs, A.; Hediger, M. A. Metal ion transporters in mammals: structure, function and pathological implications. *J. Physiol.* **1999**, *518*, 1−12. (d) Finney, L. A.; Halloran, T. V. Transition metal speciation in the cell: insights from the chemistry of metal ion receptors. *Science* **2003**, *300*, 931−936. (e) Nelson, N. Metal ion transporters and homeostasis. *EMBO J.* **1999**, *18*, 4361−4371. (f) Kozlowski, H.; Janicka-Klos, A.; Brasun, J.; Gaggelli, E.; Valensin, D.; Valensin, G. Copper, iron, and zinc ions homeostasis and their role in neurodegenerative disorders (metal uptake, transport, distribution and regulation). *Coord. Chem. Rev.* **2009**, *253*, 2665−2685. (g) Berg, J. M.; Shi, Y. The galvanization of biology: a growing appreciation for the roles of zinc. *Science* **1996**, *271*, 1081−1085. (h) Xie, X.; Smart, T. G. A physiological role for endogenous zinc in rat hippocampal synaptic neurotransmission. *Nature* **1991**, *349*, 521−524. (i) Maret, W. Zinc biochemistry, physiology, and homeostasis−recent insights and current trends. *BioMetals* **2001**, *14*, 187−190. (j) Vallee, B. L.; Falchuk, K. H. The biochemical basis of zinc physiology. *Physiol. Rev.* **1993**, *73*, 79−118.
(15) (a) Dong, W.-K.; Akogun, S. F.; Zhang, Y.; Sun, Y.-X.; Dong, X.-Y. A reversible "turn-on" fluorescent sensor for selective detection of $Zn^{2+}$. *Sens. Actuators, B* **2017**, *238*, 723−734. (b) Shayegan, H.; Farahani, Y. D.; Safarifard, V. A pillar-layer metal-organic framework as a turn-on luminescent sensor for highly selective and sensitive detection of Zn(II) ion. *J. Solid State Chem.* **2019**, *279*, 120968.
(16) (a) Chen, D.; Liu, Z.; Huang, W.; Zhao, Y.; Dong, S.; Zeng, M. Purification and characterisation of a zinc-binding peptide from oyster protein hydrolysate. *J. Funct. Foods* **2013**, *5*, 689−697. (b) Kristin, K.; Mark, A. S.; Per, K. Novel Zn2-Chelating Peptides Selected from a Fimbria-Displayed Random Peptide Library. *Appl. Environ. Microbiol.* **2001**, *67*, 5467−5473. (c) Joseph, K.-H.; Wong, M.; Todd, H.; Peter, J. R. Recent Advances in Macrocyclic Fluorescent Probes for Ion Sensing. *Molecules* **2017**, *22*, 200−218.
(17) (a) Donald, G. B.; Donald, B. Copper. *Clin. Toxicol.* **1999**, *37*, 217−230. (b) Lamichhane, J. R.; Osdaghi, E.; Behlau, F.; Köhl, J.; Jones, J. B.; Aubertot, J.-N. Thirteen decades of antimicrobial copper compounds applied in agriculture. A review. *Agron. Sustainable Dev.* **2018**, *38*, 28. (c) Schoffer, J. T.; Sauvé, S.; Neaman, A.; Ginocchio, R. Role of Leaf Litter on the Incorporation of Copper-Containing Pesticides into Soils under Fruit Production: a Review. *J. Soil Sci. Plant Nutr.* **2020**, *20*, 990−1000.
(18) Amie, K. B.; Amy, C. R. Structural Biology of Copper Trafficking. *Chem. Rev.* **2009**, *109*, 4760−4779.
(19) (a) Kaler, S. G. ATP7A-related copper transport diseases-emerging concepts and future trends. *Nat. Rev. Neurol.* **2011**, *7*, 15−29. (b) Lutsenko, S. Atp7b−/− mice as a model for studies of Wilson's disease. *Biochem. Soc. Trans.* **2008**, *36*, 1233−1238. (c) Que, E. L.; Domaille, D. W.; Chang, C. J. Metals in Neurobiology: Probing Their Chemistry and Biology with Molecular Imaging. *Chem. Rev.* **2008**, *108*, 1517−1549. (d) Savelieff, M. G.; Lee, S.; Liu, Y.; Lim, M. H. Untangling Amyloid-$\beta$, Tau, and Metals in Alzheimer's Disease.


https://doi.org/10.1021/acsomega.1c02855
*ACS Omega* 2021, 6, 24473−24483

*ACS Chem. Biol.* **2013**, *8*, 856−865. (e) Davies, P.; McHugh, P. C.; Hammond, V. J.; Marken, F.; Brown, D. R. Contribution of Individual Histidines to Prion Protein Copper Binding. *Biochemistry* **2011**, *50*, 10781−10791.

(20) (a) Satish, K.; Trivedi, A. V. A Review on Role of Nickel in the Biological System. *Int. J. Curr. Microbiol. Appl. Sci.* **2016**, *5*, 719−727. (b) *Nickel and Its Surprising Impact in Nature*; Sigel, A., Sigel, H., Sigel, R. K. O., Eds.; John Wiley & Sons Ltd.: U.K., 2007; Vol. 2. (c) Kusal, K. D.; Chandramouli, R. R.; Ishwar, B. B.; Swastika, D.; Shrilaxmi, B.; Lata, M.; Jyoti, P. K.; Biradar, M. S. Primary concept of nickel toxicity − an overview. *J. Basic Clin. Physiol. Pharmacol.* **2019**, *30*, 141−152. (d) Cempel, M.; Nikel, G. Nickel: A Review of Its Sources and Environmental Toxicology. *Pol. J. Environ. Stud.* **2006**, *15*, 375−382.

(21) (a) Giuseppe, G.; Alessia, C.; Graziantonio, L.; Maria, S. S.; Alessia, C. Nickel: Human Health and Environmental Toxicology. *Int. J. Environ. Res. Public Health* **2020**, *17*, 679. (b) Chivers, P. T.; Sauer, R. T. NikR is a ribbon-helix-helix DNA-binding protein. *Protein Sci.* **1999**, *8*, 2494−2500. (c) Dosanjh, N. S.; Michel, S. L. Microbial nickel metalloregulation: NikRs for nickel ions. *Curr. Opin. Chem. Biol.* **2006**, *10*, 123−130. (d) Hausinger, R. P.; Zamble, D. B. In *Molecular Microbiology of HeaVy Metals*; Nies, D. H., Silver, S., Eds.; Springer: Heidelberg, Germany, 2007; pp 287−320; (e) Carrington, P. E.; Chivers, P. T.; Al-Mjeni, F.; Sauer, R. T.; Maroney, M. J. Nickel coordination is regulated by the DNA-bound state of NikR. *Nat. Struct. Biol.* **2003**, *10*, 126−130. (f) Schreiter, E. R.; Sintchak, M. D.; Guo, Y.; Chivers, P. T.; Sauer, R. T.; Drennan, C. L. Crystal structure of the nickel-responsive transcription factor NikR. *Nat. Struct. Biol.* **2003**, *10*, 794−799.

(22) Chakraborty, S.; Rayalu, S. Detection of nickel by chemo and fluoro sensing technologies. *Spectrochim. Acta, Part A* **2021**, *245*, 118915.

(23) (a) Xu, Z.; Chen, X.; Kim, H. N.; Yoon, J. Sensors for the optical detection of cyanide ion. *Chem. Soc. Rev.* **2010**, *39*, 127−137. (b) Lodeiro, C.; Pina, F. Luminescent and chromogenic molecular probes based on polyamines and related compounds. *Coord. Chem. Rev.* **2009**, *253*, 1353−1383. (c) Basabe-Desmonts, L.; Reinhoudt, D. N.; Crego-Calama, M. Design of fluorescent materials for chemical sensing. *Chem. Soc. Rev.* **2007**, *36*, 993−1017. (e) de Silva, A. P.; Gunaratne, H. Q. N.; Gunnlaugsson, T.; Huxley, A. J. M.; McCoy, C. P.; Rademacher, J. T.; Rice, T. E. Signaling recognition events with fluorescent sensors and switches. *Chem. Rev.* **1997**, *97*, 1515−1566. (g) Kim, H.; Kim, K. B.; Song, E. J.; Hwang, I. H.; Noh, J. Y.; Kim, P.-G.; Jeong, K.-D.; Kim, C. Turn-on selective fluorescent probe for trivalent cations. *Inorg. Chem. Commun.* **2013**, *36*, 72−76.

(24) Jung, J. Y.; Han, S. J.; Chun, J.; Lee, C.; Yoon, J. New thiazolothiazole derivatives as fluorescent chemosensors for $Cr^{3+}$ and $Al^{3+}$. *Dyes Pigm.* **2012**, *94*, 423−426.

(25) Tang, L.; Li, F.; Liu, M.; Nandhakumar, R. Single sensor for two metal ions: Colorimetric recognition of $Cu^{2+}$ and fluorescent recognition of $Hg^{2+}$. *Spectrochim. Acta, Part A* **2011**, *78*, 1168−1172.

(26) Wang, S.; Men, G.; Zhao, L.; Hou, Q.; Jiang, S. Binaphthyl-derived salicylidene Schiff base for dual-channel sensing of Cu, Zn cations and integrated molecular logic gates. *Sens. Actuators, B* **2010**, *145*, 826−831.

(27) Swamy, K. M. K.; Kim, M.-J.; Jeon, H.-R.; Jung, J.-Y.; Yoon, J.-Y. New 7-hydroxycoumarinbased fluorescent chemosensors for Zn(II) and Cd(II). *Bull. Korean Chem. Soc.* **2010**, *31*, 3611−3616.

(28) Singh, N.; Kaur, N.; Ni Choitir, C.; Callan, J. F. A dual detecting polymeric sensor: chromogenic naked eye detection of silver and ratiometric fluorescent detection of manganese. *Tetrahedron Lett.* **2009**, *50*, 4201−4204.

(29) Wang, L.; Li, H.; Cao, D. A new photoresponsive coumarin-derived Schiff base: Chemosensor selectively for Al3+ and Fe3+ and fluorescence turn-on under room light. *Sens. Actuators, B* **2013**, *181*, 749−755.

(30) Wang, M.; Wang, J.; Xue, W.; Wu, A. A benzimidazole-based ratiometric fluorescent sensor for Cr3+ and Fe3+. *Dyes Pigm.* **2013**, *97*, 475−480.

(31) (a) Wu, C.; Wang, J.; Shen, J.; Zhang, C.; Wu, Z.; Zhou, H. A colorimetric quinoline-based chemosensor for sequential detection of copper ion and cyanide anions. *Tetrahedron* **2017**, *73*, 5715−5719. (b) Wang, W.; Wei, J.; Liu, H.; Liu, Q.; Gao, Y. A novel colorimetric chemosensor based on quinoline for the sequential detection of $Fe^{3+}$ and PPi in aqueous solution. *Tetrahedron Lett.* **2017**, *58*, 1025−1029. (c) Mahalingam, M.; Irulappan, M.; Kasirajan, G.; Palathurai Subramaniam, M.; Ramasamy, S.; Unnisa, N. Synthesis of bisbenzimidazo quinoline fluorescent receptor for Fe2+ ion in the aqueous medium - An experimental and theoretical approach. *J. Mol. Struct.* **2015**, *1099*, 257−265. (d) Kia, Y.; Osman, H.; Suresh Kumar, R.; Basiri, A.; Murugaiyah, V. Synthesis and discovery of highly functionalized mono- and bis-spiro-pyrrolidines as potent cholinesterase enzyme inhibitors. *Bioorg. Med. Chem. Lett.* **2014**, *24*, 1815−1819. (e) Karmakar, M.; Bhatta, S. R.; Giri, S.; Thakur, A. Oxidation induced differentially selective turn-on fluorescence via photoinduced electron transfer based on a ferrocene-appended coumarin-quinoline platform: Application in cascaded molecular logic. *Inorg. Chem.* **2020**, *59*, 4493−4507.

(32) (a) Minyan, H.; Jintao, Z.; Xudong, Z.; Yuzhe, Z.; Song, X.; Zhongyu, L. Novel spiropyran derivative based reversible photo-driven colorimetric and fluorescent probes for recognizing Fe3+, Cr3+ and Al3+ metal ions. *Inorg. Chem. Commun.* **2020**, *117*, 107968. (b) Kiani, M.; Bagherzadeh, M.; Meghdadi, S.; Rabiee, N.; Abbasi, A.; Schenk-Joß, K.; Tahriri, M.; Tayebi, L.; Webster, T. J. Development of a Novel Carboxamide-Based Off-On Switch Fluorescence Sensor: Hg2+, Zn2+ and Cd2+. *New J. Chem.* **2020**, *44*, 11841. (c) Uahengo, V.; Hamukwaya, E. N.; Endjala, P. T.; Naimhwaka, J. H. A potential naphthyl-thiazole-based organic dye and a ditopic chromogenic probe for CN- and Fe3+ with molecular logic functions. *New J. Chem.* **2020**, *44*, 18588. (d) Salman, A. K. Multi-step synthesis, photophysical and physicochemical investigation of novel pyrazoline a heterocyclic D- p -A chromophore as a fluorescent chemosensor for the detection of Fe3p metal ion. *J. Mol. Struct.* **2020**, *1211*, 128084. (e) Zixuan, Y.; Yaqiang, T.; Sheng, C.; Leiyu, Z.; Liang, L. The synthesis of a series of fluorescent emitters and their application for dye lasing and cation sensing. *Spectrochim. Acta, Part A* **2021**, *246*, 118978. (f) Ammar, R. A.; Alturiqi, A. S.; Alaghaz, A.-N. M. A.; Zayed, M. E. Synthesis, spectral characterization, quantum chemical calculations, in-vitro antimicrobial and DNA activity studies of 2-(2 '-mercaptophenyl) benzothiazole complexes. *J. Mol. Struct.* **2018**, *1168*, 250−263. (g) Daravath, S.; Kumar, M. P.; Rambabu, A.; Vamsikrishna, N.; Ganji, N.; Shivaraj. Design, synthesis, spectral characterization, DNA interaction and biological activity studies of copper(II), cobalt(II) and nickel(II) complexes of 6-amino benzothiazole derivatives. *J. Mol. Struct.* **2017**, *1144*, 147−158. (h) Tian, X.; Zhao, Y.; Li, Y.; Yang, C.; Zhou, Z. Sensitive and selective ratiometric nanosensors for visual detection of Cu2+ based on ions promoted oxidation reaction. *Sens. Actuators, B* **2017**, *247*, 139−145. (i) Jadhao, M.; Das, C.; Rawat, A.; Kumar, H.; Joshi, R.; Maiti, S.; Ghosh, S. K. Development of multifunctional heterocyclic Schiff base as a potential metal chelator: a comprehensive spectroscopic approach towards drug discovery. *JBIC, J. Biol. Inorg. Chem.* **2017**, *22*, 47−59. (j) Sharma, A. K.; Kim, J.; Prior, J. T.; Hawco, N. J.; Rath, N. P.; Kim, J.; Mirica, L. M. Small Bifunctional Chelators That Do Not Disaggregate Amyloid beta Fibrils Exhibit Reduced Cellular Toxicity. *Inorg. Chem.* **2014**, *53*, 11367−11376. (k) Gulcan, M.; Karataş, Y.; Işık, S.; Öztürk, G.; Akbaş, E.; Şahin, E. Transition Metal(II) Complexes of a Novel Symmetrical Benzothiazole-Based Ligand: Synthesis, Spectral/Structural Characterization and Fluorescence Properties. *J. Fluoresc.* **2014**, *24*, 1679−1686. (l) Barreto, J.; Venkatachalam, T. K.; Joshi, T.; Kreher, U.; Forsyth, C. M.; Reutens, D.; Spiccia, L. Synthesis, characterization and coordination chemistry of aminophenylbenzothiazole substituted 1,4,7-triazacyclononane macrocycles. *Polyhedron* **2013**, *52*, 128−138. (m) Banci, L.; Bertini, I.; Durazo, A.; Girotto, S.; Gralla, E. B.; Martinelli, M.; Valentine, J. S.; Vieru, M.; Whitelegge, J. P. Metal-free superoxide dismutase forms soluble oligomers under physiological conditions: A possible general mechanism for familial ALS. *Proc. Natl. Acad. Sci. U.S.A.* **2007**, *104*, 11263−11267.



https://doi.org/10.1021/acsomega.1c02855
*ACS Omega* 2021, 6, 24473−24483

(33) Dennis, R.; Ludger, S.; Victor, B.; Frank, R.; Michael, M. Synthesis of para-Aryl-Substituted Salicyldialdehydes. *Eur. J. Org. Chem.* **2015**, 3274−3285.
(34) Chaitali, V. M.; Jayashree, D. Review of heavy metals in drinking water and their effect on human health. *Int. J. Innov. Res. Sci., Eng. Technol.* **2013**, *7*, 2992−2996.
(35) Frisch, M. J.; Trucks, G. W.; Schlegel, H. B.; Scuseria, G. E.; Robb, M. A.; Cheeseman, J. R.; Scalmani, G.; Barone, V.; Mennucci, B.; Petersson, G. A.; Nakatsuji, H.; Caricato, M.; Li, X.; Hratchian, H. P.; Izmaylov, A. F.; Bloino, J.; Zheng, G.; Sonnenberg, J. L.; Hada, M.; Ehara, M.; Toyota, K.; Fukuda, R.; Hasegawa, J.; Ishida, M.; Nakajima, T.; Honda, Y.; Kitao, O.; Nakai, H.; Vreven, T.; Montgomery, J. A.; Peralta, J. E., Jr.; Ogliaro, F.; Bearpark, M.; Heyd, J. J.; Brothers, E.; Kudin, K. N.; Staroverov, V. N.; Keith, T.; Kobayashi, R.; Normand, J.; Raghavachari, K.; Rendell, A.; Burant, J. C.; Iyengar, S. S.; Tomasi, J.; Cossi, M.; Rega, N.; Millam, J. M.; Klene, M.; Knox, J. E.; Cross, J. B.; Bakken, V.; Adamo, C.; Jaramillo, J.; Gomperts, R.; Stratmann, R. E.; Yazyev, O.; Austin, A. J.; Cammi, R.; Pomelli, C.; Ochterski, J. W.; Martin, R. L.; Morokuma, K.; Zakrzewski, V. G.; Voth, G. A.; Salvador, P.; Dannenberg, J.; Dapprich, S.; Daniels, A. D.; Farkas, O.; Foresman, J. B.; Ortiz, J. V.; Cioslowski, J.; Fox, D. J. *Gaussian 09*, Revision B.01; Gaussian, Inc.: Wallingford CT, 2010.
(36) (a) Qi, W.; Li, H. F.; Jian, B. C.; Yu, W.; Shaomin, S. Ratiometric sensing of Zn2+ with a new benzothiazole-based fluorescent sensor and living cell imaging. *Analyst* **2021**, *146*, 4348−4356. (b) Suman, G. R.; Bubbly, S. G.; Gudennavar, S. B.; Gayathri, V. Benzimidazole and benzothiazole conjugated Schiff base as fluorescent sensors for Al3+ and Zn2+. *J. Photochem. Photobiol., A* **2019**, *382*, 1119472. (c) Mayank, G.; Sunanda, S.; Vivekanand, S.; Parimal, K. B. Benzothiazole integrated into a cryptand for ESIPT-based selective chemosensor for Zn2+ ions. *Dalton Trans.* **2019**, *48*, 7801−7808. (d) Suparna, P.; Priyabrata, B. An ESIPT based turn on fluorochromogenic sensor for low level discrimination of chemically analogous Zn2+ and Cd2+ & aqueous phase recognition of bio-hazardous CN-: From solution state analysis to prototype fabrication. *Sens. Actuators, B* **2021**, *329*, 129172. (e) Zheng, L.; Jing, W.; Liwei, X.; Jiayu, W.; Hanlei, Y. A dual-response fluorescent probe for Al3+ and Zn2+ in aqueous medium based on benzothiazole and its application in living cells. *Inorg. Chim. Acta* **2021**, *516*, 120147. (f) Begum, T.; Hayder, M. A. A.; Serkan, E. Fast and Reversible "Turn on" Fluorescent Sensors Based on Bisphenol-a for $Zn^{2+}$ in Aqueous Solution. *J. Fluoresc.* **2019**, *29*, 1079−1087. (g) Barbara, P.; Rosita, D.; Simona, C.; Lucia, S.; Angela, T.; Stefano, P.; Ugo, C. Fluorescence pH-dependent sensing of Zn(II) by a tripodal ligand. A comparative X-ray and DFT study. *J. Lumin.* **2019**, *212*, 200−206.


https://doi.org/10.1021/acsomega.1c02855
*ACS Omega* 2021, 6, 24473−24483